

NOTES AND CORRESPONDENCE

On the Crucial Role of Basin Geometry in Double-Gyre Models of the Kuroshio Extension

STEFANO PIERINI

Dipartimento di Scienze per l'Ambiente, Università di Napoli Parthenope, Naples, Italy

(Manuscript received 1 October 2007, in final form 6 November 2007)

ABSTRACT

The decadal chaotic relaxation oscillation obtained in a recent double-gyre model study of the Kuroshio Extension intrinsic low-frequency variability was found to compare surprisingly well with the real variability of the jet as revealed by altimeter data, despite the high degree of idealization of the model. In this note it is shown that elements of realism in the basin geometry, present in that study and absent in previous double-gyre models applied to the Kuroshio Extension, play a crucial role in shaping the low-frequency variability of the jet, and can explain the good performance of the model. A series of numerical experiments with different basin geometries of increasing degrees of simplicity are analyzed. If the schematic western boundary representing the coastline south of Japan is removed, the strong decadal variability completely disappears and only a very weak periodic oscillation about an elongated state of the jet is found. If the large zonal width of the basin (representing correctly the extension of the North Pacific Ocean) is reduced by a half, then the total meridional Sverdrup transport is reduced by the same factor, and so is the intensity of the Kuroshio and Oyashio western boundary currents: as a result, the modeled Kuroshio Extension is totally unrealistic in shape and is steady. If both simplifications are introduced the resulting jet is, again, totally unrealistic, yielding a weak periodic bimodal cycle. On the basis of these results, two main conclusions are drawn: (i) the introduction of appropriate geometrical elements of realism in double-gyre model studies of the Kuroshio Extension is essential, and (ii) the Kuroshio Extension intrinsic low-frequency variability would be dramatically different if the southwestern coastline of Japan were more meridionally oriented.

1. Introduction

The mean jet and the low-frequency variability obtained with a “double-gyre model” (e.g., Dijkstra 2005; Dijkstra and Ghil 2005) of the Kuroshio Extension (Pierini 2006, hereafter P06) were recognized to be in significant agreement with both in situ and altimetric measurements. The meandering pattern of the modeled mean jet yields two main crests and other secondary features in very good agreement with the climatological surface dynamic height of Teague et al. (1990), as discussed in detail in section 3b of P06. The modeled low-frequency variability is characterized by a decadal chaotic relaxation oscillation that connects a zonally elongated, fairly stable, energetic meandering jet and a

much weaker, very unstable jet with a reduced zonal penetration. These high and low energy states are found to be quantitatively very similar to the “elongated” and “contracted” states known to occur in the Kuroshio Extension (e.g., Qiu 2000). More specifically, (i) the characteristic decadal period, (ii) the evolution of the mean latitudinal position and (iii) of the path-length of the meandering jet during a typical bimodal cycle, (iv) the more stable character of the elongated state compared to the contracted state, and (v) the spatial patterns and their temporal sequence obtained by the model are all found to be in significant quantitative agreement—within the limits of an idealized model—with the altimeter data presented by Qiu and Chen (2005), derived by merging the Ocean Topography Experiment [(TOPEX)/Poseidon], *Jason-1*, and the *European Remote Sensing Satellite-1/2* (ERS-1/2) measurements for the period 1992–2004 (see section 4b of P06 for a detailed comparison between modeling results and altimeter data).

Corresponding author address: Stefano Pierini, Dipartimento di Scienze per l'Ambiente, Università di Napoli Parthenope, Centro Direzionale–Isola C4, 80143 Naples, Italy.
E-mail: stefano.pierini@uniparthenope.it

Two comments can be made on the basis of this successful experimental validation. The first is that this result supports the hypothesis that the observed Kuroshio Extension (KE) low-frequency variability is primarily due to intrinsic nonlinear mechanisms internal to the ocean system rather than being induced, directly or indirectly, by an analogous atmospheric variability, although it is obvious that the latter does affect in many important ways the oceanic response at all spatial and temporal scales. The second comment, which motivates this note, concerns the reason why this double-gyre model implementation was so successful in reproducing in a quantitatively correct way the most relevant features of the KE decadal variability, while previous double-gyre models did not prove to be as successful to this respect.

In fact, the classical rectangular box double-gyre problem has played a fundamental role in the investigation of the internal low-frequency variability of the large-scale midlatitude ocean circulation, putting forward the innovative hypothesis that intrinsic nonlinear oceanic mechanisms can, in some significant cases, be responsible for observed large-scale low-frequency ocean changes; moreover, the same modeling studies have contributed substantially to disseminate in the context of physical oceanography the concepts and methods of nonlinear dynamical systems and bifurcation theory. However, to the best of the author's knowledge, direct and detailed comparison of idealized double-gyre model results with experimental data was never even attempted before P06 for the KE, although results of other double-gyre models were nonetheless found in some cases to represent *qualitatively* the observed KE low-frequency variability.

As an example of this limitation let us consider the recent model study by Primeau and Newman (2008, hereafter PN08; see also Primeau 2002 for an analogous quasigeostrophic model). The authors developed a double-gyre model that has many features in common with that of P06: they are both based on the reduced-gravity shallow-water equations, the steady wind stress fields used are comparable, and the hydrological and dissipative parameters differ, but not in a very significant way; nonetheless the results are very different. By applying both continuation methods and forward-time integrations, PN08 found that, for a given range of the viscosity parameter, a stable steady state (corresponding to a strong and deeply penetrating jet, interpreted as a paradigm of the KE elongated state) and a chaotic attractor (corresponding to a weaker and less penetrating variable jet, interpreted as a paradigm of the KE contracted state) coexist, but they are disconnected. To this respect the authors conjecture that some time de-

pendence of the wind could induce transitions between the two states. On the other hand, in P06 the elongated and contracted states are in much better agreement with the observed ones; moreover, the fairly realistic decadal chaotic transition between them (interpreted as a homoclinic orbit in phase space) is spontaneously produced by a steady wind, without the need of any time dependence in the forcing. Why? In other terms, the question is the following: What difference in the model implementation can account for such a macroscopic difference in the results of these two models that, after all, are so similar?

In this note we will show that elements of realism in the geometry of the domain of integration play a crucial role in the generation of the intrinsic low-frequency variability in double-gyre models of the Kuroshio Extension, and can well account for the different performance of the two model studies in the example quoted above, since in P06 such elements of realism were present while they were absent in the other model implementation. It is important to emphasize that, in this note, when we refer to *elements of realism in the geometry* we do not have in mind a domain that is bounded by a realistic coastline (in which case we would be outside a process study approach typical of the double-gyre problem), but rather to schematic geometrical features, whose insertion in the model does not modify its mechanistic nature (a fundamental characteristic for studies aimed at understanding dynamical processes), but can nonetheless have a profound effect on the degree of realism of the results.

In section 2 the flows produced with the same model of P06 but with four different geometries, each differing from the more realistic geometry adopted by P06 (denoted B0) for some relevant detail, are compared with the flow obtained with B0 and discussed on the basis of geophysical fluid dynamics and the dynamical systems' theory. Finally, in section 3 conclusions are drawn.

2. Sensitivity numerical experiments with different basin geometries

In the model study of P06 the initial boundary value problem for the reduced-gravity shallow-water equations is solved, starting from rest, in the domain of integration, denoted here as B0, shown in Fig. 1. For all the technical details and parameter values used, the reader should refer to the original paper. Following the "poor man's continuation method" (Dijkstra and Ghil 2005), also imposed by the very large dimension of the domain of integration, several sensitivity experiments were performed in P06 by varying the lateral eddy viscosity coefficient K_H and the forcing amplitude α (see

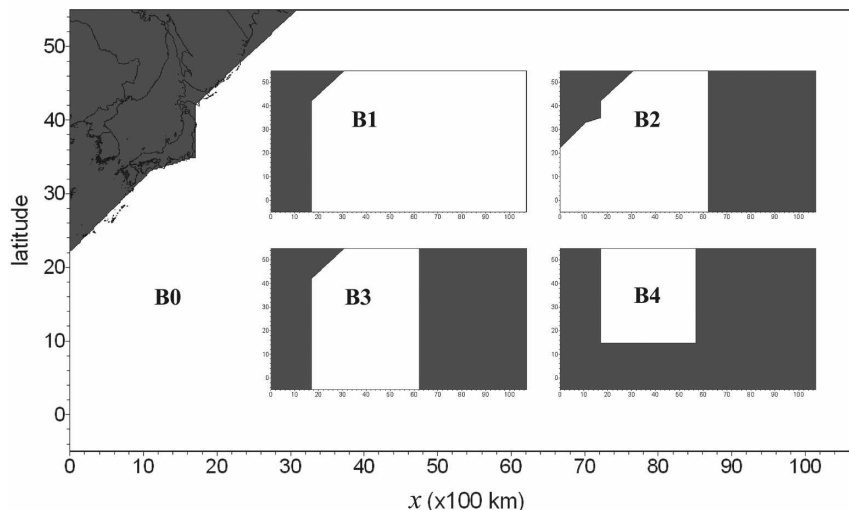


FIG. 1. The basin geometries used in the numerical experiments (the boxes of geometries B1–B4 are reduced in size to fit inside the large box of geometry B0). Geometry B0 is the one adopted by P06.

P06, his section 1b) about a “basic” (and most realistic) case, for which $K_H = 220 \text{ m}^2 \text{ s}^{-1}$ and $\alpha = 1$, with the aim of analyzing the properties of the solutions in terms of dynamical systems theory (DST). However, in this note the four numerical experiments presented in sections 2b–e differ from the basic case *only* for a different basin geometry, all the other parameters and technical details remain exactly the same, except from sensitivity experiments in which K_H is varied, whose results are,

however, not shown but only summarized in the discussion. The time series of the kinetic energy (per unit mass) of the KE jet integrated in the sector Ω (defined by the rectangle reported in Fig. 3a) for the five cases B0–B4 are shown in Fig. 2 for a 100-yr integration. Before analyzing the solutions obtained with the new geometries, in section 2a we need to recall some important properties of the basic case presented in P06.

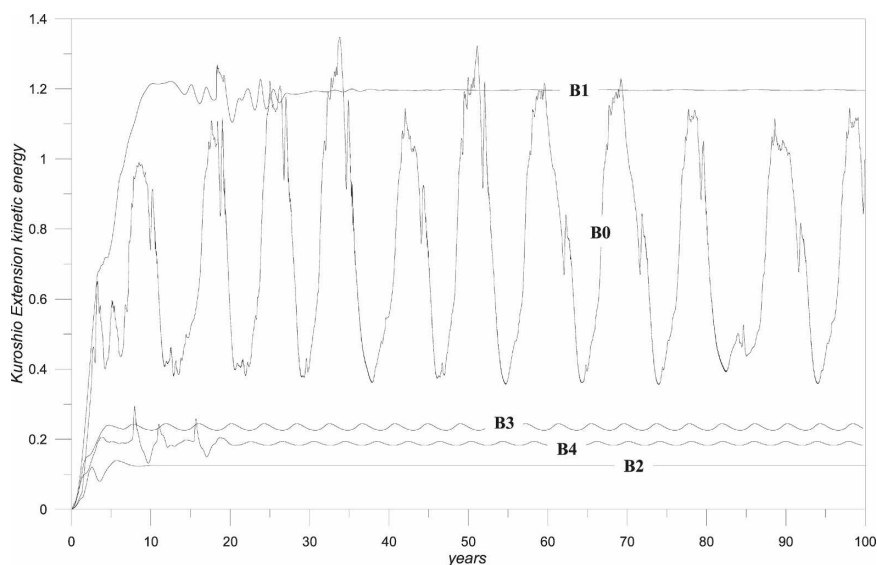


FIG. 2. Time series of the kinetic energy per unit mass ($10^{13} \text{ m}^5 \text{ s}^{-2}$; integrated over the sector Ω) of the modeled Kuroshio Extension for the various geometries.

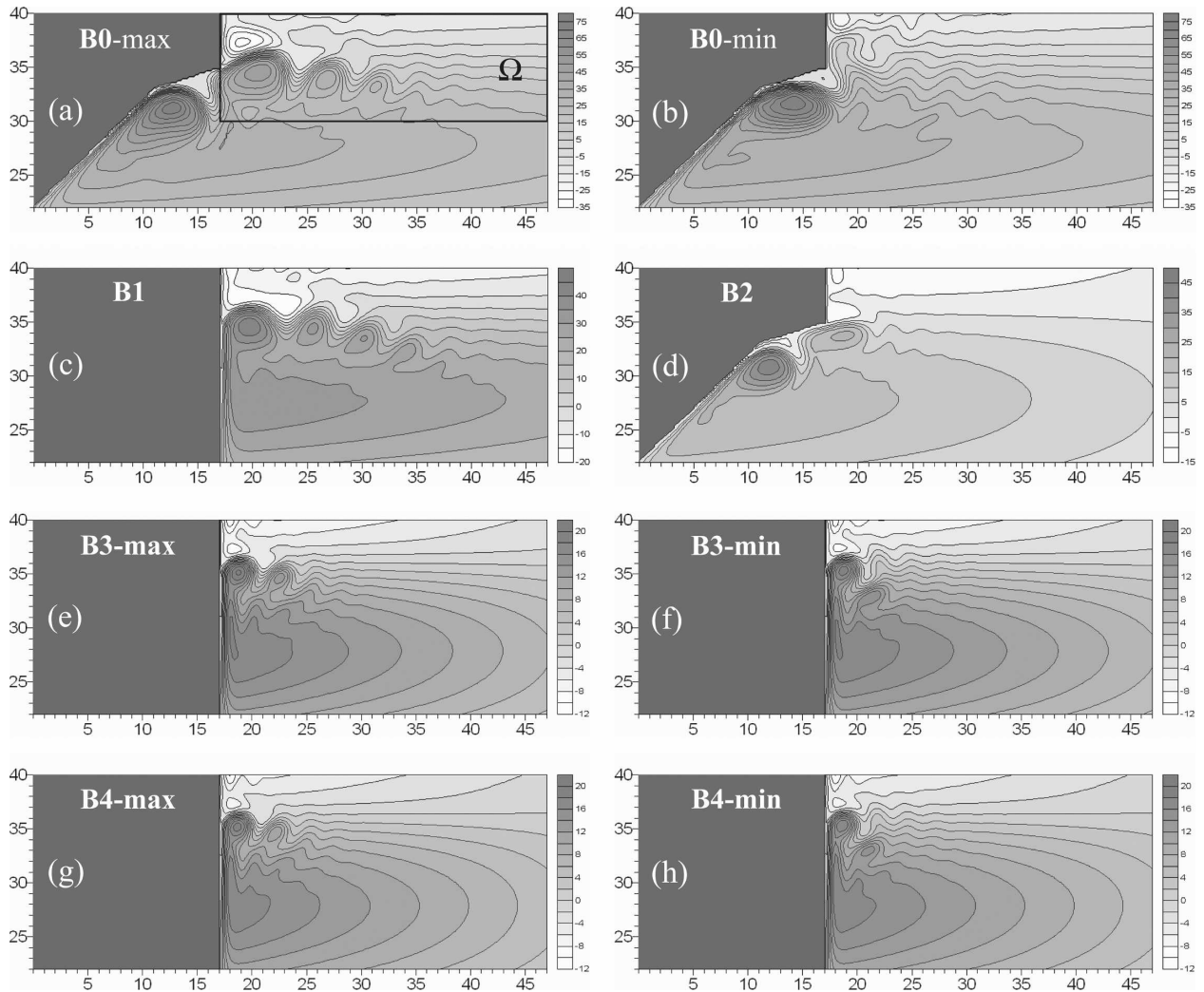


FIG. 3. Sea surface displacement (cm), in a window covering the Kuroshio Extension region, for the various basin geometries. For geometries B0, B3, and B4 the two panels correspond to the maximum and minimum energy states of the corresponding bimodal cycle; (a), (b) are adapted from P06.

a. The most realistic domain (B0)

The large-amplitude decadal bimodal chaotic oscillation of case B0 shown in Fig. 2 connects an elongated and a contracted state, as reported in Figs. 3a,b (corresponding to the snapshots at $t = 143$ yr and $t = 148$ yr of P06, respectively). The dynamical interpretation proposed in P06 of the relaxation oscillation associated with such a bimodal cycle is now summarized (see P06 for further details).

The KE in Fig. 3a (which we assume corresponding here to $t' = 0$, where $t' \equiv t - 143$ yr) is in the highest energy elongated state and in a fairly stable phase; a strong stable anticyclonic recirculation gyre and a cyclonic meander farther east are present south of Japan. In the next ~ 2 yr the amplitude of the KE jet slightly

decreases: this is because the flux of negative relative vorticity coming from the south is balanced by dissipation in the region south of Japan due to the locally very strong horizontal gradients: as a consequence, the KE jet cannot be fed by an analogous input of vorticity, so it is slowly weakened by dissipation. A critical transition occurs when, at $t' \sim 3$ yr, the weakening of the first KE crest allows the erosion of the cyclonic meander south of Japan. This disrupts the stable phase and leads to the intensification of the Kuroshio recirculation gyre, which eventually assumes a straight path that penetrates into the open sea. During the next year, the recirculation gyre moves back south of Japan, leaving a very weak KE jet northeast of it.

We are now at $t' = 5$ yr (Fig. 3b), when the energy is at its minimum and the recharging of the KE begins.

From now on the KE intensifies being fed by the flux of negative relative vorticity coming from the south, which, in this phase, can overcome the southern recirculation gyre because dissipation cannot balance it locally. In the last ~ 2 yr of the recharging phase ($t' = 9\text{--}10$ yr) the intensification is accompanied by the ejection of cold-core eddies detaching from a meridionally elongated cyclonic meander (a process well known to occur south of Japan; e.g., Qiu and Miao 2000).

From the point of view of DST such relaxation oscillation is interpreted as a homoclinic orbit associated with the reconnection of the stable and unstable manifolds of the saddle fixed point corresponding to the weak jet state (virtually equal to the state shown in Fig. 3b). The occurrence of homoclinic orbits in the double-gyre problem was elucidated by Nadiga and Luce (2001) and Simonnet et al. (2005).

b. Domain with a meridional coastline south of Japan (B1)

In P06 it is mentioned (without presenting the results) that the schematic coastline plays an extremely important role, and that its absence drastically modifies the response. Let us therefore consider geometry B1 (Fig. 1), which differs from B0 only in that the schematic coastline south of Japan is substituted by a straight meridional line. This modification is apparently a minor one, yet its effect on the oceanic response is absolutely dramatic since the strong bimodal variability obtained with B0 completely disappears in this case. Figure 2 shows that after spinup the trajectory is attracted by a very small amplitude limit cycle (of period $T = 9.55$ yr), whose energy is roughly equal to the maximum value attained in the chaotic oscillations of case B0. Figure 3c shows the pattern of the flow, which remains virtually unchanged during the weak periodic oscillation. It resembles the elongated state—east of Japan—of case B0 (Fig. 3a), with a squeezed main meander and the other meanders slightly shifted to the west (the detachment from the coast is $\sim 2^\circ$ south of the line of vanishing wind stress curl, that in our case is $\varphi = 37^\circ\text{N}$). As we have seen in section 2a, the relaxation oscillation of case B0 is strictly related to the existence of the anticyclonic recirculation gyre and the cyclonic meander south of Japan, which obviously require a northern inclined coastline south of 35°N . Thus, eliminating this geometrical feature makes the relaxation oscillation disappear. From the DST point of view this can be expressed by saying that the homoclinic relaxation oscillation is promoted by the north–south asymmetry in the flow induced by the Japanese coastline, and that its absence modifies the structure of phase

space so profoundly that no global bifurcation occurs and only weak gyre modes arise.

In this respect it is interesting to notice that numerical experiments (not shown), in which K_H is decreased, show evidence that the elongated jet of Fig. 3c is very robust under variations of the lateral eddy viscosity coefficient. Indeed, even a remarkable decrease of this dissipation parameter (up to $K_H \approx 100 \text{ m}^2 \text{ s}^{-1}$), while leading to a larger and larger mean energy level and to chaotic oscillations of increasing amplitude, leaves the meandering jet unaltered in its basic structure, the low-frequency variability only introducing minor modifications in the flow. This is a striking example of how nonlinearities are able to sustain extremely stable large-scale coherent structures.

c. Domain with a reduced zonal extension (B2)

For a given wind stress field, the extension of the basin determines the total meridional Sverdrup transport and, consequently, the transports of the northward and southward western boundary currents whose confluence gives rise to the free extension jet. Thus, if geometry B2 (in which the zonal extension east of Japan is half of the one in case B0) is adopted, the total input of momentum is reduced by about 50%, so the transports of the modeled Kuroshio and Oyashio Currents are, in turn, expected to be reduced by a factor ~ 0.5 with respect to the basic case B0; this should produce dramatic changes in the response since we are in a parameter range in which nonlinear effects are extremely strong. This is indeed the case, as shown by Figs. 2 and 3d. The obtained flow is steady and the KE is very weak and totally unrealistic.

This sensitivity experiment is probably trivial, but it nonetheless points to the importance of choosing a basin geometry with a correct zonal extension in the double-gyre model approach, if looking for an oceanic response that yields realistic features. In fact, too often the relevance of such a requirement is underestimated (e.g., this reduced zonal extension is, to our knowledge, roughly equal to the maximum extension ever used in previous double-gyre model studies, and if this is definitely acceptable for applications to the Gulf Stream, it does not appear to be the case for the KE).

d. Domain with a meridional coastline south of Japan and with a reduced zonal extension (B3)

In basins B1 and B2 two geometric features (a schematic but relatively realistic western coastline and a correct zonal extension) are separately removed from geometry B0. In geometry B3 both features are removed. In Fig. 2 it is interesting to see that, despite the

unrealistically small flow transport common to cases B2 and B3, with B3 the KE undergoes a weak but significant periodic bimodal oscillation (with period $T = 4.2$ yr), while it is steady with B2. This is because the system anticyclonic recirculation gyre–cyclonic meander allowed in B2 by the presence of the coastline south of Japan has a stabilizing effect, like in the stable phase of case B0, while its absence in B3 allows for a weak relaxation oscillation (totally different from the one described in section 2a) shown in Figs. 3e,f. The first, main meander remains virtually unchanged while the smaller one to the east undergoes a meridional oscillation and intensifies when it reaches the highest latitude.

e. Small rectangular domain (B4)

In the last sensitivity experiment a rectangular basin (B4) is considered, with a zonal extension of 4000 km and a latitudinal extension of 4448 km (40°). This domain is basically the one adopted by many authors in studying the Gulf Stream low-frequency variability and also by PN08 to study the KE (but their meridional width was only 2800 km). Consistently with the lack of any geometrical asymmetry, in this run the zonal dependence of the wind stress forcing present in the previous cases (see section 2b of P06) is now eliminated, but this has only a minor effect on the result. The oceanic response is very similar to the one obtained with geometry B3 (the period of the bimodal cycle is now $T = 4$ yr), as shown in Figs. 2 and 3g,h. This is not surprising, the total Sverdrup transport being virtually the same, since the lower zonal boundary is located at $\varphi = 15^\circ\text{N}$ (i.e., south of the southern line of vanishing wind stress curl at $\varphi = 18^\circ\text{N}$); moreover, the inclined western boundary north of 42°N , now absent, plays a minor role in the oceanic response (but it is worth noticing that its presence in the geometries with full zonal length B0 and B1 is necessary in order to avoid instabilities that would arise north of the KE with a meridional—and luckily less realistic—coastline).

To analyze the dependence of the oceanic response under variations of the dissipation parameter, a series of runs (not shown) have been performed with decreasing value of K_H . As a result, the structure of the jet is found to be very robust under such variations. For values smaller than $K_H = 220 \text{ m}^2 \text{ s}^{-1}$ the flow soon becomes chaotic; for even smaller values up to $K_H = 120 \text{ m}^2 \text{ s}^{-1}$ the range of variation of the kinetic energy of the jet increases moderately, but in all cases the bimodality shown in Figs. 3g,h remains substantially unaltered. Below this value, the system yields instabilities associated with the expulsion from the jet of very energetic vortex pairs that move northward.

It is worth noticing that the zonal extension of the jet,

which is 700–800 km, and its meandering pattern are both comparable to the contracted jet of PN08 located on their A' branch, as could be expected in advance by considering the similarity of both dynamical model and geometry used in the two model approaches. On the other hand, an important difference emerges as well: while in PN08 for sufficiently small viscosity a run started from rest leads, after spinup, to chaotic oscillations about an elongated state (on their C' branch after the first Hopf bifurcation H_C ; e.g., see Fig. 7 of PN08), here the solution for B4, also starting from rest, adjusts to the contracted state for any admissible value of K_H , as described above, and no elongated state arises (obviously, such a state may well exist in some region of phase space for some value of K_H , but finding it with our empirical continuation method would require starting the run from an initial condition belonging to its basin of attraction, an initial guess that is unfortunately lacking). In any case, the similarity of these two contracted states supports the conjecture that if the model of PN08 were extended to include a sufficiently large zonal extension (B4 \rightarrow B1) necessary to provide the correct input of momentum, and a Japanese coastline (B1 \rightarrow B0) necessary for the formation of a realistic relaxation oscillation, then a global bifurcation could take place, and a homoclinic orbit connecting a contracted and an elongated state similar to that obtained by P06 would arise.

3. Conclusions

In this note we have shown that the classical rectangular box double-gyre model of the wind-driven ocean circulation with a zonal extension of at most ~ 4000 km (typical of previous studies) cannot reproduce a low-frequency variability of the Kuroshio Extension in agreement with observations. On the contrary, a double-gyre model, forced by a fairly realistic wind forcing, whose domain of integration has a schematic but relatively realistic coastline southwest of Japan and a zonal width of ~ 9000 km (representing correctly the extension of the North Pacific Ocean) does yield a decadal relaxation oscillation, corresponding to a homoclinic orbit in phase space, in significant agreement with altimeter observations. The reason why these two geometric elements of realism can dramatically affect the modeled KE low-frequency variability has been elucidated through a series of numerical experiments with different basin geometries.

On the basis of these results, a first conclusion can be drawn: the introduction of appropriate geometrical features in double-gyre models of the Kuroshio Extension is absolutely essential if any comparison with observations is the goal, since the regime of low-frequency vari-

ability in basic agreement with observations is found to be extremely sensitive to specific details of the continental geometry. Another conclusion that may have paleoclimatic implications is that the Kuroshio Extension's low-frequency variability would be dramatically different if the southwestern coastline of Japan were more meridionally oriented.

Although the results presented in this note apply to the Kuroshio Extension, some considerations can be made in relation to the Gulf Stream extension case. In an application of the double-gyre problem to the North Atlantic, Dijkstra and Molemaker (1999) have shown that the perturbed pitchfork bifurcation found in a rectangular basin remains robust if more realistic geometries (either the real coastline or sloping western and eastern boundaries) are considered. This suggests that the intrinsic low-frequency variability of the Gulf Stream and of its extension is much less sensitive to the basin geometry than it is the case for the KE. This may be partly due to the lack, in the western North Atlantic, of strong coastline variations such as those present in the western North Pacific, which in turn may be the cause of a less pronounced bimodality of the Gulf Stream extension compared to that of the KE. Nevertheless, the sensitivity numerical experiments presented in this note may stimulate analogous studies for the North Atlantic, where in general the role of basin geometry on the intrinsic low-frequency variability has probably not received sufficient attention.

Acknowledgments. I am pleased to thank Henk A. Dijkstra for valuable discussions and for his useful comments on the manuscript.

REFERENCES

- Dijkstra, H. A., 2005: *Nonlinear Physical Oceanography: A Dynamical Systems Approach to the Large Scale Ocean Circulation and El Niño*. Springer, 532 pp.
- , and M. J. Molemaker, 1999: Imperfections of the North Atlantic wind-driven ocean circulation: Continental geometry and windstress shape. *J. Mar. Res.*, **57**, 1–28.
- , and M. Ghil, 2005: Low-frequency variability of the large-scale ocean circulation: A dynamical systems approach. *Rev. Geophys.*, **43**, RG3002, doi:10.1029/2002RG000122.
- Nadiga, B. T., and B. P. Luce, 2001: Global bifurcation of Shilnikov type in a double-gyre ocean model. *J. Phys. Oceanogr.*, **31**, 2669–2690.
- Pierini, S., 2006: A Kuroshio Extension system model study: Decadal chaotic self-sustained oscillations. *J. Phys. Oceanogr.*, **36**, 1605–1625.
- Primeau, F., 2002: Multiple equilibria and low-frequency variability of the wind-driven ocean circulation. *J. Phys. Oceanogr.*, **32**, 2236–2256.
- , and D. Newman, 2008: Elongation and contraction of the Western Boundary Current extension in a shallow-water model: A bifurcation analysis. *J. Phys. Oceanogr.*, in press.
- Qiu, B., 2000: Interannual variability of the Kuroshio Extension system and its impact on the wintertime SST field. *J. Phys. Oceanogr.*, **30**, 1486–1502.
- , and W. Miao, 2000: Kuroshio path variations south of Japan: Bimodality as a self-sustained internal oscillation. *J. Phys. Oceanogr.*, **30**, 2124–2137.
- , and S. Chen, 2005: Variability of the Kuroshio Extension jet, recirculation gyre, and mesoscale eddies on decadal time scales. *J. Phys. Oceanogr.*, **35**, 2090–2103.
- Simonnet, E., M. Ghil, and H. A. Dijkstra, 2005: Homoclinic bifurcations in the quasi-geostrophic double-gyre circulation. *J. Mar. Res.*, **63**, 931–956.
- Teague, W. J., M. J. Carron, and P. J. Hogan, 1990: A comparison between the Generalized Digital Environmental Model and Levitus climatologies. *J. Geophys. Res.*, **95**, 7167–7183.